^{21}Ne(^{3}He,p)^{23}Na reaction

H. T. Fortune,* J. R. Powers,† and R. Middleton
Physics Department, University of Pennsylvania, Philadelphia, Pennsylvania 19104

H. Nann‡ and B. H. Wildenthal
Cyclotron Laboratory, Michigan State University, East Lansing, Michigan 48823

(Received 24 March 1978)

The reaction ^{21}Ne(^{3}He,p) ^{23}Na has been investigated at a bombarding energy of 18.0 MeV, using enriched ^{21}Ne gas contained in a rotating gas cell. Angular distributions for the positive-parity states have been analyzed with the distorted-wave Born approximation, using transfer amplitudes from an $(sd)^7$ shell-model calculation. Agreement with experiment is good. Tentative correspondences are suggested for all experimental and theoretical levels below 6 MeV excitation. Low-lying negative-parity states are very weakly populated.

[NUCLEAR REACTIONS ^{21}Ne(^{3}He,p), $E=18.0$ MeV; measured $\sigma(E_p,\theta)$. ^{23}Na deduced levels L, J, π. DWBA analysis with shell-model wave functions. Enriched gas target.]

I. INTRODUCTION

The most severe critique of existing nuclear shell-model theory is its ability to predict correctly observables for nuclei in the middle of a shell.

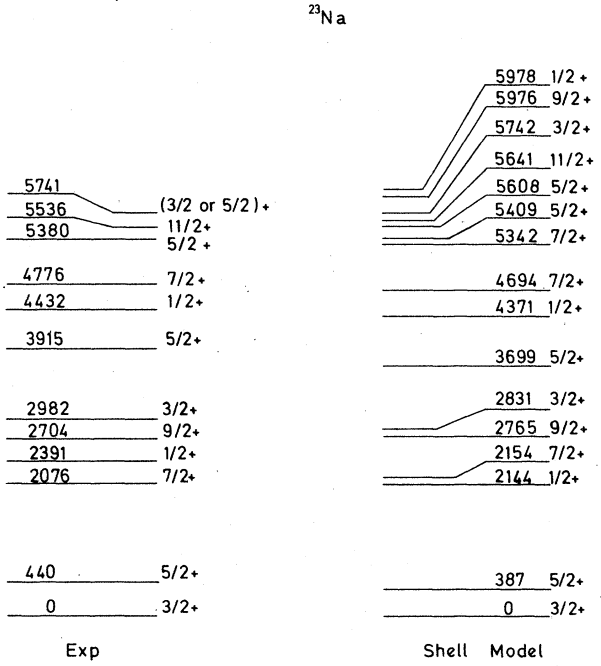

FIG. 1. Experimental levels of ^{23}Na (left, Ref. 1) known to have positive parity prior to present work compared with energies calculated in an $(sd)^7$ basis (right, Ref. 2). Only levels below 6 MeV are included.

A rather sensitive test of the wave functions of the initial and final states can be provided by the comparison of experimental two-nucleon transfer differential cross sections with microscopic distorted-wave Born approximation (DWBA) calculations based on matrix elements of the coupled two-particle creation (or annihilation) operator.

In the case of the reaction under study here ^{21}Ne(^{3}He,p)^{23}Na, most of the levels in the final nucleus ^{23}Na below 6 MeV of excitation have known[1] spin and parity. All of them that are known to have even parity can be identified with states predicted in an $(sd)^7$ shell-model calculation.[2] Except for a $K^\pi=\frac{7}{2}^+$ rotational band that is predicted, but not observed, the agreement between calculated and measured energies is very good, as depicted in Fig. 1.

Spectroscopic amplitudes calculated from the wave functions of Ref. 2 were used with DWBA calculations to predict the shapes and relative differential cross sections of transitions to even parity states in ^{23}Na. The ability to reproduce the shape of the experimental angular distributions and the consistency of the ratio of the measured and calculated cross sections then give a measure of the goodness of the theoretical wave functions.

II. EXPERIMENTAL PROCEDURE AND RESULTS

The experiment was performed with an 18-MeV ^{3}He beam from the University of Pennsylvania tan-

dem accelerator. Gas enriched to 86.5% in ^{21}Ne was enclosed in a rotating gas cell.[3] The cell window was 522 μg/cm^2 Mylar. Outgoing protons were momentum analyzed in a multiangle spectrograph and recorded on nuclear emulsion plates. Absorber foils placed directly in front of the focal planes stopped all particles except protons. Data were recorded in 7.5° intervals from 7.5° to 60°. The long run time necessary because of small cross sections (collected charge was 5 000 μC) created experimental difficulties. Heat produced by the beam passage through the Mylar window partially evaporated the window material and also created small holes in the window, resulting in contamination by nitrogen, oxygen, and carbon compounds, and a slow loss of Ne gas.

Since the gas pressure could be measured only when filling the cell, a Si surface-barrier detector recorded elastically scattered ^{3}He ions to continuously monitor the condition of the target gas. Monitor spectra were recorded in 100-μC intervals and provided a means of calculating the average pressure over the entire run—this was 30 Torr, corresponding to an effective ^{21}Ne target thickness of 33 μg/cm^2. In addition to C, N, and O impurities, nonnegligible amounts of ^{20,22}Ne were also present in the target gas. A spectrum is displayed in Fig. 2. Level numbers correspond to those in Tables I and II. Below 6 MeV excitation, the impurities presented a problem only for very weak states. Above that energy, the problem was more severe. Hence, we restrict our attention to levels below 6 MeV. Experimental resolution averaged 42 keV, full width at half maximum (FWHM), and arose primarily from straggling of the ^{3}He ions in the relatively thick cell window and the changing gas pressure.

Average excitation energies obtained in the present work are compared with results from the literature in Tables I and II. Overall agreement is good. States with obvious shell-model counterparts are listed in Table I, additional levels in Table II. Negative-parity states at 2.64, 3.68, and 3.85 MeV were very weak, as expected from their predominant hole structure. Levels 14, 15, and 16 at excitation energies of[1] 5741, 5766, and 5781 keV were not resolved, but the average excitation energy extracted for the triplet suggests that most

TABLE I. Results of the reaction ^{21}Ne (^{3}He, p) ^{23}Na for states with obvious shell-model counterparts.

Literature[a]		Present work		Theory[b]	$N = \sigma_{exp}/\sigma_{th}$[c]	
J^π	E_x (keV)	Level no.	E_x (keV)	E_x (keV)	pot'l (*N*,*N*)	pot'l (4,1)
$\frac{3}{2}^+$	0.0	0	0.0	0.0	210	250
$\frac{5}{2}^+$	439.9 ± 0.2	1	443 ± 3	387	335	405
$\frac{7}{2}^+$	2076.4 ± 0.3	2	2072 ± 6	2154	190	225
$\frac{1}{2}^+$	2390.9 ± 0.3	3	2390 ± 6	2144	640	900
$\frac{9}{2}^+$	2703.7 ± 0.4	5	2703 ± 6	2765	200	225
$\frac{3}{2}^+$	2982.4 ± 0.2	6	2984 ± 5	2831	470	550
$\frac{5}{2}^+$	3914.7 ± 0.5	9	3913 ± 4	3699	360	400
$\frac{1}{2}^+$	4432.0 ± 0.8	10	4429 ± 4	4371	360	440
$\frac{7}{2}^+$	4775.6 ± 0.5	11	4772 ± 4	4694	290	300
$\frac{11}{2}^+$	5536 ± 4	13	5542 ± 4[d]	5641	(1200)	(1400)
					340	410

[a] Reference 1.
[b] Reference 2.
[c] Computed as described in the text, with potential combinations listed in Table III, and transfer amplitudes in Table IV.
[d] Suggested herein to contain an unresolved state with $J^\pi = (\frac{3}{2}, \frac{5}{2}, \frac{1}{2})^+$.

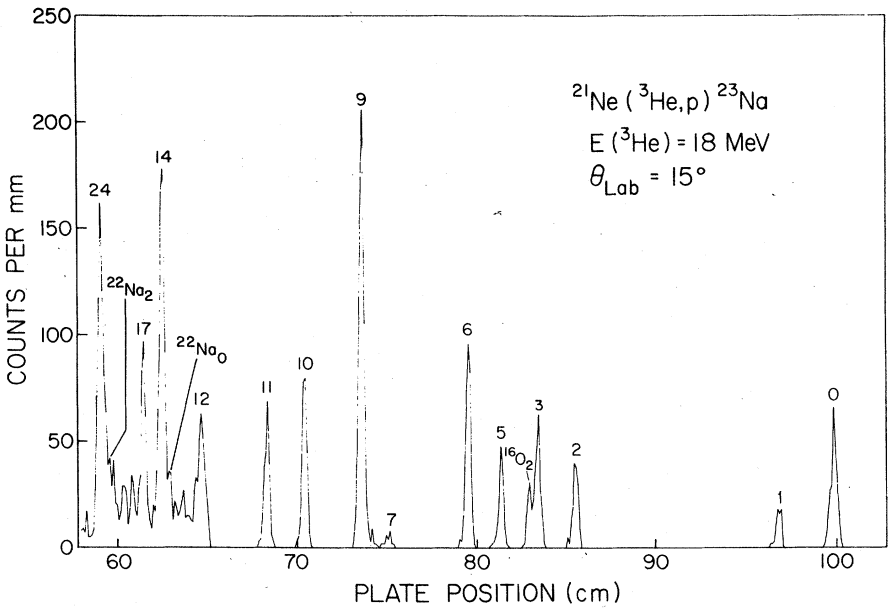

FIG. 2. Spectrum of the ^{21}Ne(^{3}He,p)^{23}Na reaction at a bombarding energy of 18.0 MeV and a laboratory angle of 15°. Level numbers correspond to those in Tables I and II.

TABLE II. Results of the ^{21}Ne (^{3}He, p) ^{23}Na reaction for additional levels below 6 MeV excitation.

Literature[a]		Present work			
J^π	E_x (keV)	Level no.	E_x (keV)	L	Remarks
$\frac{1}{2}^-$	2639.8 ± 0.3	4	2640 ±10	...	Very weak
$\frac{3}{2}^-$	3678.3 ± 0.4	7	3678 ± 4	1 + 3	
$\frac{5}{2}^-$	3848.2 ± 0.8	8	3855 ± 6	1 + 3	
$\frac{5}{2}^+(\frac{3}{2}^+)$[b]	5380 ± 2	12	5375 ±10	2 (+0)	Probably $\frac{5}{2}^+_3$ s.m. state
$(\frac{5}{2},\frac{3}{2})^+$[c]	5740.7 ± 1.1	14	5743 ±10	0 (+ higher L)	Probably $\frac{5}{2}^+_4$ s.m. state
$\frac{1}{2}(\frac{3}{2})$[d]	5766.3 ± 1.1	15			One member probably $\frac{1}{2}^+$
$\frac{1}{2}(\frac{3}{2})$[d]	5781 ± 8	16			
$(\frac{7}{2},\frac{5}{2})$[e]	5931 ± 4	17	5927 ±12	(2)	Probably $\frac{7}{2}^+$
$(\frac{1}{2},\frac{3}{2})^-$	5967 ± 2	18			

[a] From Reference 1, unless otherwise noted.
[b] $\frac{5}{2}^+$ preferred (References 4, 5).
[c] $\frac{5}{2}^+$ preferred (Reference 4).
[d] From Reference 5. If $J^\pi(5741) = \frac{5}{2}^+$, both have $J = \frac{1}{2}$.
[e] From Reference 5.

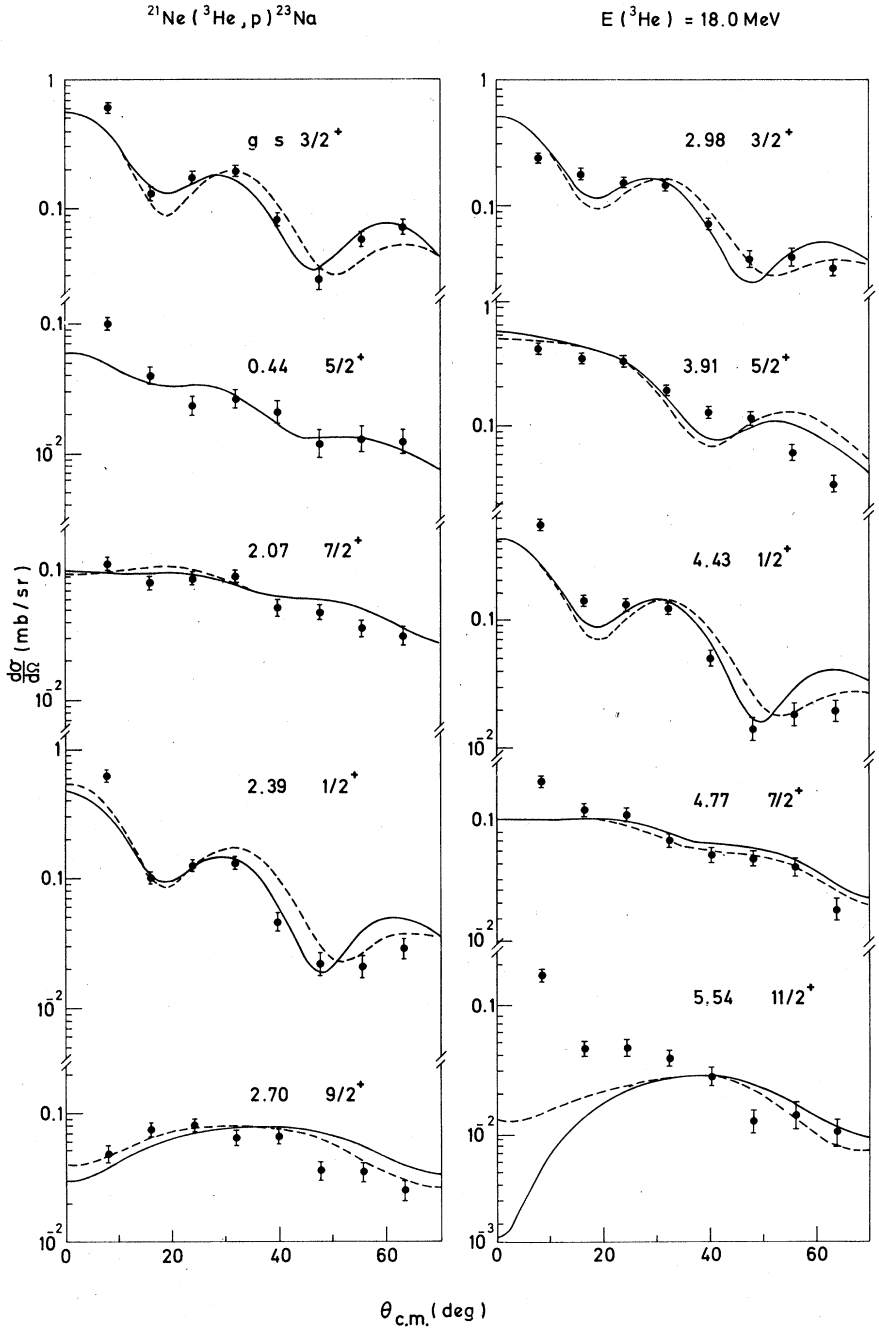

FIG. 3. Angular distributions for the ^{21}Ne(^{3}He,p)^{23}Na reaction leading to levels of ^{23}Na whose identifications with shell-model states are clear. Curves are results of DWBA calculations, using optical-model parameters listed in Table III [solid, set (N,N); dashed, set (4, 1)] and transfer amplitudes listed in Table IV. Resulting normalization factors σ_{exp}/σ_{th} are given in Table I.

of the cross section arises from the lowest member, which has $J^{\pi} = (\frac{3}{2}^+, \frac{5}{2}^+)$, with $\frac{5}{2}^+$ strongly preferred.[4,5] Likewise, levels 17 and 18 at 5931 and 5967 were not resolved, but the lower appears much stronger. Angular distributions are presented in Figs. 3 and 4, where they are compared with DWBA curves as discussed in the next section.

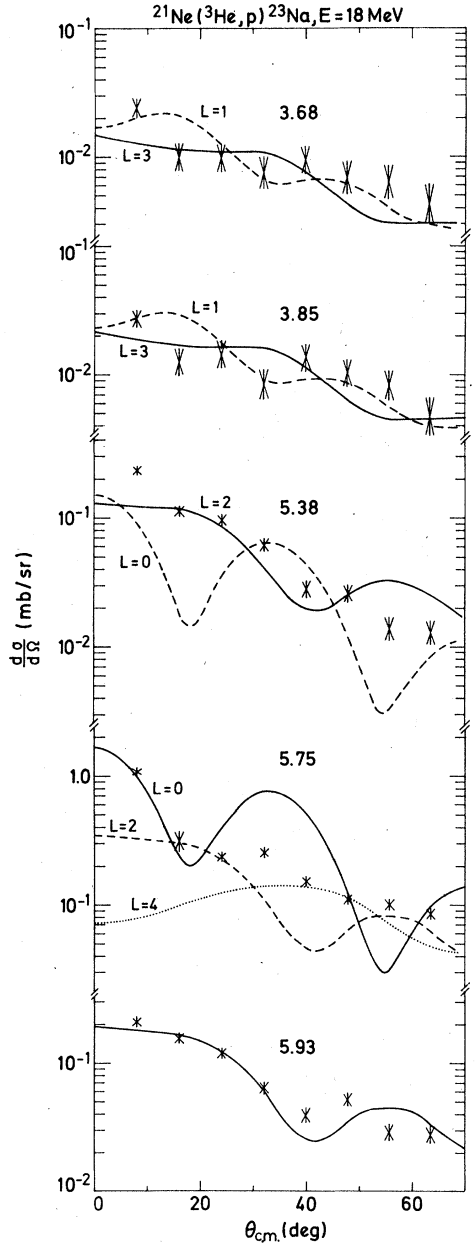

FIG. 4. Angular distributions for the ^{21}Ne(^{3}He,p)^{23}Na reaction for additional levels below 6 MeV excitation. Curves are results of pure-configuration DWBA calculations for L values indicated, using pot'l set (4,1) of Table III.

III. ANALYSIS AND DISCUSSION

Theoretical angular distributions were calculated with the DWBA code DWUCK,[6] using two different sets of optical-model parameters taken from the literature,[7-9] which are listed in Table III. For states with obvious shell-model counterparts (those listed in Table I), two-nucleon transfer amplitudes calculated from the shell-model wave functions of Ref. 2 were used. These amplitudes are listed in Table IV. Theoretical cross sections are defined as

$$\sigma_{\rm th}(\theta) = N \frac{2J_f+1}{2J_i+1} \sum_{LSTJ} b_{ST}{}^2 D_{ST}{}^2 (T_i T_{zi} TO \,|\, T_f T_{zf})^2 \times \frac{(2S+1)}{(2J+1)} \sigma_{\rm DWUCK}(\theta).$$

The sum is over the transferred spin and isospin S, T and transferred orbital and total angular momentum L, J. Selection rules for a (^{3}He,p) reaction require $T=1$ for $S=0$, and vice versa. The quantity $(T_i T_{zi} TO \,|\, T_f T_{zf})^2$ is the square of a Clebsch-Gordan coefficient, $(\frac{1}{2}\frac{1}{2} TO \,|\, \frac{1}{2}\frac{1}{2})^2$, connecting the isospin of the initial and final states; $b_{ST}{}^2 = \frac{1}{2}$ for both values of S, T. We have used $D_{10}{}^2 = 0.30$, $D_{01}{}^2 = 0.72$ (see Ref. 10). The quantities J_f, J_i are the final and initial angular momentum, respectively.

These theoretical curves were normalized to the data as displayed in Fig. 3, resulting in the normalization factors N listed in Table I. The solid curves were calculated with the potential pair (N,N) of Table III, and the dashed curves with the pair (4,1). The principal difference between calculations with the two potential sets is the relative ratio of $L=0$ and 2. The average ratio $N = \sigma_{\rm exp}/\sigma_{\rm th}$, ignoring the $\frac{11}{2}^+$ state (to which we return below), is 340 for potential set (N,N) and 410 for potential set (4,1). Fluctuations about the average value are about a factor of 2 in either direction. A systematic analysis[11] of (t,p) reactions, but without the factor $D_{01}{}^2 = 0.72$, yielded $N = 310$. So we would expect $N = 310/0.72 = 430$, within a factor of 2 of most of our ratios. Thus, the shell-model wave functions do very well in accounting for the magnitude of the ^{21}Ne(^{3}He,p) cross section.

The wave functions correctly predict the dominance of $L=4$ for the lowest $\frac{7}{2}^+$ and $\frac{9}{2}^+$ state, though $L=2$ is also allowed for both, and correctly predict the dominance of $L=2$ for the $\frac{5}{2}^+$ state at 3.91 MeV. For the latter, the shell model predicts virtually no $L=0$, and in fact none is observed. Theoretical curves for $L=0$ do not have as much of a forward peak as the data exhibit, but the model correctly predicts $L=0$ dominance for the g.s. and the lowest two $\frac{1}{2}^+$ states. It fails slightly in predicting too little $L=0$ for the 0.44-MeV $\frac{5}{2}^+$ state and 4.77-MeV $\frac{7}{2}^+$ state and not enough for the 2.98-MeV $\frac{3}{2}^+$ level. Nevertheless, overall the agreement is as good as usually encountered in (^{3}He,p) reactions.

We return now to the $\frac{11}{2}^+$ state at 5.54 MeV. The selection rules allow only $L=4$ for this state, and

TABLE III. Optical-model parameters used in analysis of ^{21}Ne (^{3}He, p). (Potentials in MeV, lengths in fm.)

Channel	Label	V	r_0	a	W	$W' = 4W_D$	r_0'	a'	V_{so}	r_{oc}
^{3}He	N[a]	162.9	1.16	0.69	17.9	0	1.50	0.82	0	1.25
	4[b]	170	1.14	0.723	20	0	1.60	0.80	0	1.4
P	N[a]	54.0	1.25	0.65	0	60	1.25	0.47	0	1.25
	1[b]	54.6	1.123	0.57	0	33.6	1.123	0.50	5.5	1.4
Bound	N[a]	...	1.25	0.65	...	...	...	...	$\lambda = 25$	1.25
state	1[b]	...	1.26	0.60	...	...	...	...	$\lambda = 25$	1.26

[a] See References 7 and 8.
[b] See Reference 9.

TABLE IV. Spectroscopic amplitudes for ^{21}Ne → ^{23}Na.

E_x (MeV)					Amplitudes[c]				
Exp[a]	Th[b]	J^{π}[a]	J	T	$(1d_{5/2})^2$	$(1d_{5/2})(2s_{1/2})$	$(1d_{5/2})(1d_{3/2})$	$(2s_{1/2})^2$	$(2s_{1/2})(1d_{3/2})$	$(1d_{3/2})^2$
0.0	0.0	$\frac{3}{2}^+$	0	1	0.8577			0.1952		0.3408
			1	0	-0.3063		0.2034	-0.0332	0.0571	0.0090
			2	0	0	0.0501	-0.0298		0.0348	
			2	1	-0.0629	0.0178	-0.1802		0.0598	-0.0193
			3	0	0.5450	-0.1001	-0.1754			-0.0938
0.44	0.39	$\frac{5}{2}^+$	1	0	-0.1050		0.1130	0.0024	0.0223	-0.0095
			2	0	0	-0.0259	0.0005		-0.0135	
			2	1	-0.2241	0.0744	-0.2436		0.0842	-0.0647
			3	0	-0.0427	-0.0177	0.1876			-0.0395
			4	0	0		0.2004			
			4	1	-0.1781		-0.0043			
2.07	2.15	$\frac{7}{2}^+$	2	0	0	0.0210	-0.0066		-0.0077	
			2	1	0.3406	-0.1939	0.1720		-0.1241	0.0708
			3	0	-0.4235	-0.0016	-0.0373			0.1044
			4	0	0		0.1676			
			4	1	0.4336		0.1580			
			5	0	0.5195					
2.39	2.14	$\frac{1}{2}^+$	1	0	0.2283		-0.4900	0.0920	0.1732	-0.0992
			2	0	0	-0.0002	-0.2200		0.1000	
			2	1	-0.1549	0.1168	-0.2343		-0.0209	-0.1731
2.70	2.76	$\frac{9}{2}^+$	3	0	0.1789	-0.0889	0.0598			-0.0629
			4	0	0		0.0498			
			4	1	-0.4305		-0.0979			
			5	0	0.5956					
2.98	2.83	$\frac{3}{2}^+$	0	1	0.0941			0.0293		0.0426
			1	0	-0.2156		0.3563	-0.0765	-0.0549	0.1110
			2	0	0	0.2054	-0.1019		0.0374	
			2	1	-0.1426	0.0927	-0.1919		-0.0347	-0.1389
			3	0	0.1300	-0.0300	-0.2283			0.1281
3.91	3.70	$\frac{5}{2}^+$	1	0	-0.0387		0.0798	0.0448	0.0014	0.0420
			2	0	0	0.0906	0.1564		-0.0426	
			2	1	-0.1104	0.1063	-0.0226		0.1316	0.0409
			3	0	0.1475	-0.4594	-0.0983			0.0148
			4	0	0		0.0867			
			4	1	-0.2039		-0.2993			

TABLE IV. (*Continued*)

E_x (MeV)					Amplitudes[c]					
Exp[a]	Th[b]	J^{π}[a]	J	T	$(1d_{5/2})^2$	$(1d_{5/2})(2s_{1/2})$	$(1d_{5/2})(1d_{3/2})$	$(2s_{1/2})^2$	$(2s_{1/2})(1d_{3/2})$	$(1d_{3/2})^2$
4.43	4.37	$\frac{1}{2}^+$	1	0	0.4079		-0.4067	0.1387	0.1067	-0.1042
			2	0	0	0.0011	-0.3514		0.0289	
			2	1	-0.4280	0.1741	-0.2366		0.0604	-0.1428
4.77	4.69	$\frac{7}{2}^+$	2	0	0	-0.0234	-0.0442		0.0321	
			2	1	-0.0510	0.0593	0.0205		0.0506	0.0154
			3	0	-0.1093	0.1029	0.2553			-0.1041
			4	0	0		-0.3887			
			4	1	-0.1171		-0.3452			
			5	0	-0.0086					
5.54	5.64	$\frac{11}{2}^+$	4	0	0		-0.0288			
			4	1	0.2016		0.0625			
			5	0	0.0655					

[a] Reference 1.
[b] Reference 2.
[c] Phases correct for DWUCK input.

yet an $L=4$ curve gives a poor account of the measured angular distribution, which appears to contain appreciable components of $L=0$ and 2. The cross section is also much larger than predicted. In a recent study of the reaction ^{19}F(^{6}Li,d)^{23}Na,[12] the angular distribution for this level was also much more forward peaked than expected for an $\frac{11}{2}^+$ state. The possibility thus presents itself that this level is actually an unresolved doublet. The presence of $L=0$ would imply $J^{\pi}=(\frac{1}{2}-\frac{5}{2})^+$ for the other member. Additional presence of $L=2$ does not restrict the spin further. It is interesting that the shell-model calculations (Fig. 1) predict two $\frac{5}{2}^+$ levels, a $\frac{3}{2}^+$ and a $\frac{1}{2}^+$ level between 5 and 6 MeV. One of the $\frac{5}{2}^+$ levels undoubtedly corresponds to the 5.38-MeV level discussed below. An additional level, at 5.74 MeV, is known to have $J^{\pi}=\frac{3}{2}^+$ or $\frac{5}{2}^+$. Thus in the experimental spectrum, a $\frac{1}{2}^+$ state and either a $\frac{3}{2}^+$ or $\frac{5}{2}^+$ state is missing. We suggest that one of these is unresolved from the $\frac{11}{2}^+$ state.

Levels without obvious shell-model counterparts are listed in Table II, and their angular distributions are displayed in Fig. 4, where they are compared with pure-configuration DWBA curves. The 2.64-MeV $\frac{1}{2}^-$ state is extremely weak, and the presence of an impurity peak from ^{14}N(^{3}He,p) prevents extraction of a reliable angular distribution for it. The $\frac{3}{2}^-$ and $\frac{5}{2}^-$ levels at 3.68 and 3.85 MeV, respectively, are also weak, but their angular distributions can be fitted with admixtures of $L=1$ and 3.

Level 12, at 5.38 MeV, has an angular distribution that is dominated by $L=2$, but with a small $L=0$ component, consistent with the supposed $J^{\pi}=\frac{5}{2}^+$ for this state. Level 14, at 5.74 MeV, is known to have $J^{\pi}=\frac{3}{2}^+$ or $\frac{5}{2}^+$, with $\frac{5}{2}^+$ preferred. The other two members of the triplet must have low spin $\frac{1}{2}$ and $\frac{1}{2}$ or $\frac{1}{2}$ and $\frac{3}{2}$. If $J^{\pi}(5.74)=\frac{5}{2}^+$, they must both have $J=\frac{1}{2}$, as discussed in Ref. 5. The angular distribution for the triplet has a large $L=0$ component, but with an admixture of a higher L value. One of the two $J=\frac{1}{2}$ states could be the $\frac{1}{2}^+$ state predicted near here.

The level at 5.93 MeV has $J=\frac{5}{2}$ or $\frac{7}{2}$ from[5] ^{25}Mg(d,α), with parity undetermined. The 5.97-MeV state has $J^{\pi}=(\frac{1}{2},\frac{3}{2})^-$. The combined angular distribution appears to be dominated by $L=2$, which would imply positive parity for the 5.93-MeV level. The absence of a stripping pattern in (^{3}He,d) would favor $\frac{7}{2}^+$ (Ref. 4). If both the 5.38- and 5.74-MeV levels are $\frac{5}{2}^+$, then combining all the available data suggests that the state that is unresolved from the $\frac{11}{2}^+$ at 5.54 MeV has $J^{\pi}=\frac{3}{2}^+$, and one of the 5.76- or 5.78-MeV levels has $J^{\pi}=\frac{1}{2}^+$, leaving only a $\frac{7}{2}^+$ shell-model state with no experimental counterpart. The 5.93-MeV level might be it.

IV. CONCLUSION

Experimental differential cross sections for transitions to even parity states in the ^{21}Ne(^{3}He,p)^{23}Na reaction are reproduced quite well with microscopic single-step DWBA calculations based on spectroscopic amplitudes calculated from the full sd shell basis wave functions of Ref. 2. For all the shell-model states predicted below 6 MeV of excitation, experimental counterparts could

be suggested taking all available information into account. As expected, the odd parity states in ^{23}Na which have predominant hole configurations are only weakly excited.

Financial support was provided by the National Science Foundation. We are grateful to G. Stephans for his assistance in the data analysis.

---

*Present address: KVI, Groningen, on leave from University of Pennsylvania.
†Present address: IDA, 400 Army-Navy Drive, Arlington, Virginia 22202.
‡Present address: LAMPF, Los Alamos, New Mexico 87545.

[1]P. M. Endt and C. van der Leun, Nucl. Phys. A214, 1 (1973).
[2]W. Chung and B. H. Wildenthal (unpublished).
[3]P. Neogy, R. Middleton, and W. Scholz, Phys. Rev. C 6, 885 (1972).
[4]J. R. Powers, H. T. Fortune, R. Middleton, and O. Hansen, Phys. Rev. C 4, 2030 (1971).
[5]J. R. Powers, H. T. Fortune, and R. Middleton, Nucl. Phys. A298, 1 (1978).
[6]P. D. Kunz (unpublished).
[7]E. R. Flynn, O. Hansen, and O. Nathan, Nucl. Phys. A228, 189 (1974).
[8]F. Perey, Phys. Rev. 131, 745 (1965).
[9]J. D. Garrett, R. Middleton, D. J. Pullen, S. A. Anderson, and O. Nathan, Nucl. Phys. A164, 449 (1971); H. T. Fortune, T. J. Gray, W. Trost, and N. R. Fletcher, Phys. Rev. 179, 1033 (1969); B. A. Watson, P. P. Singh, and R. E. Segel, *ibid.* 182, 977 (1969).
[10]J. C. Hardy and I. S. Towner, Phys. Lett. 25B, 98 (1967).
[11]E. R. Flynn and O. Hansen, Phys. Lett. 31B, 135 (1970).
[12]H. T. Fortune *et al.*, this issue, Phys. Rev. C 18, 255 (1978).